



Comparison of forcings of oceanic deep convection between the Irminger and Mediterranean Seas

G. Caniaux¹, *R. Waldman*¹, A. Piron², V. Thierry², H. Mercier³, H. Giordani¹

¹ CNRM, Météo France / CNRS, Toulouse, France

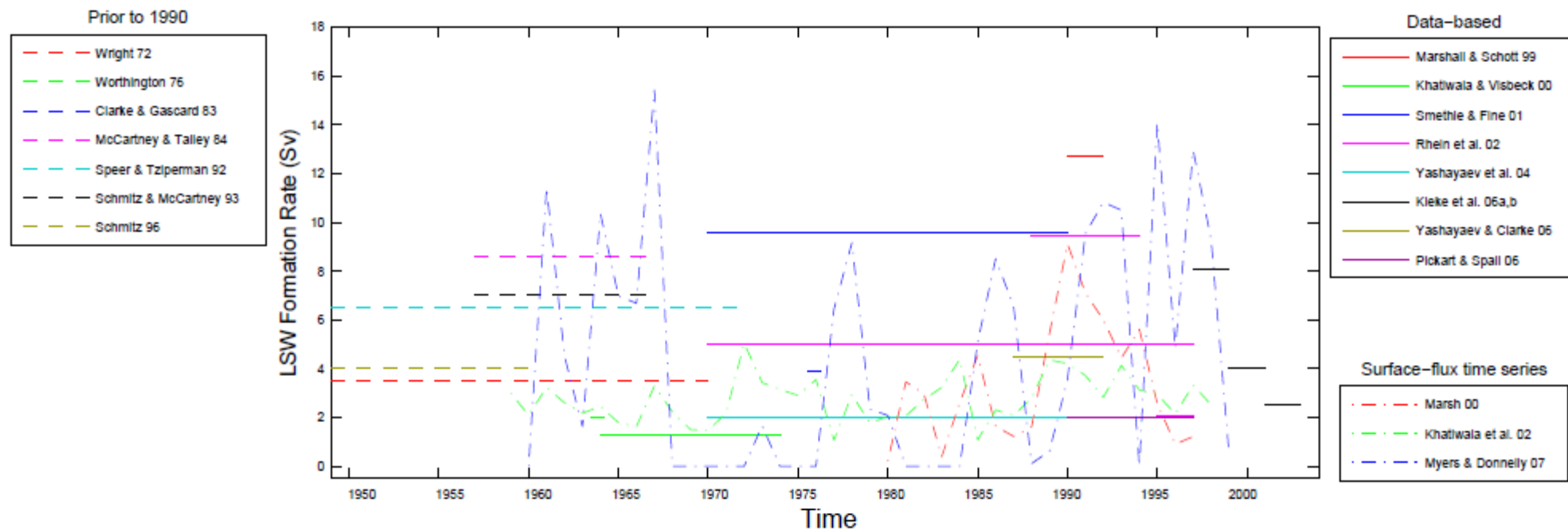
² LOPS/CNRS, Plouzané, France

³ LOPS/IFREMER, Plouzané, France

Deep convection feeds the downwelling branch of the AMOC

Estimates of the Labrador Sea deep convection rate

Haine et al 2008



Estimates of the Northwestern Mediterranean Sea deep convection rate

Waldman et al 2016

Period	Estimates From Observations
Climatological mean	1.56 Sv <i>Bethoux</i> [1980], salinity budgets
1991–1992	1 Sv <i>Tziperman and Speer</i> [1994], surf. diapycnal mixing (29 kg/m ³)
2004–2006 average	1.22 Sv <i>Rhein</i> [1995], box biogeochemical model inversion
2011–2012	0.3 Sv <i>Marshall and Schott</i> [1999], mixed patch estimate
2012–2013	1.2 Sv <i>Schroeder et al.</i> [2008b], quantitative (θ , S) diagram
	1.1 Sv <i>Durrieu de Madron et al.</i> [2013], satellite ocean color data
	1.4 ± 0.3 Sv or 2.3 ± 0.5 Sv (this study), diapycnal mixing (29.11 kg/m ³)

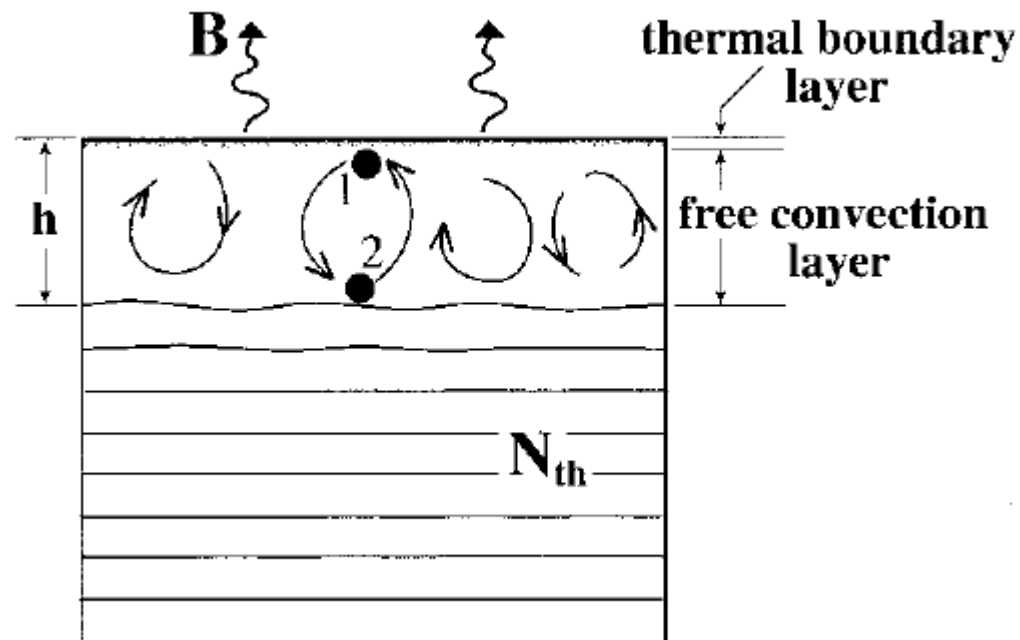
→ Ocean deep convection is still a poorly documented phenomenon

The paradigm of upright deep convection

- Mechanism = gravitational instability
- Return to equilibrium = upward transfer of buoyancy by mixed layer deepening

Scheme of upright deep convection

Marshall and Schott 1999

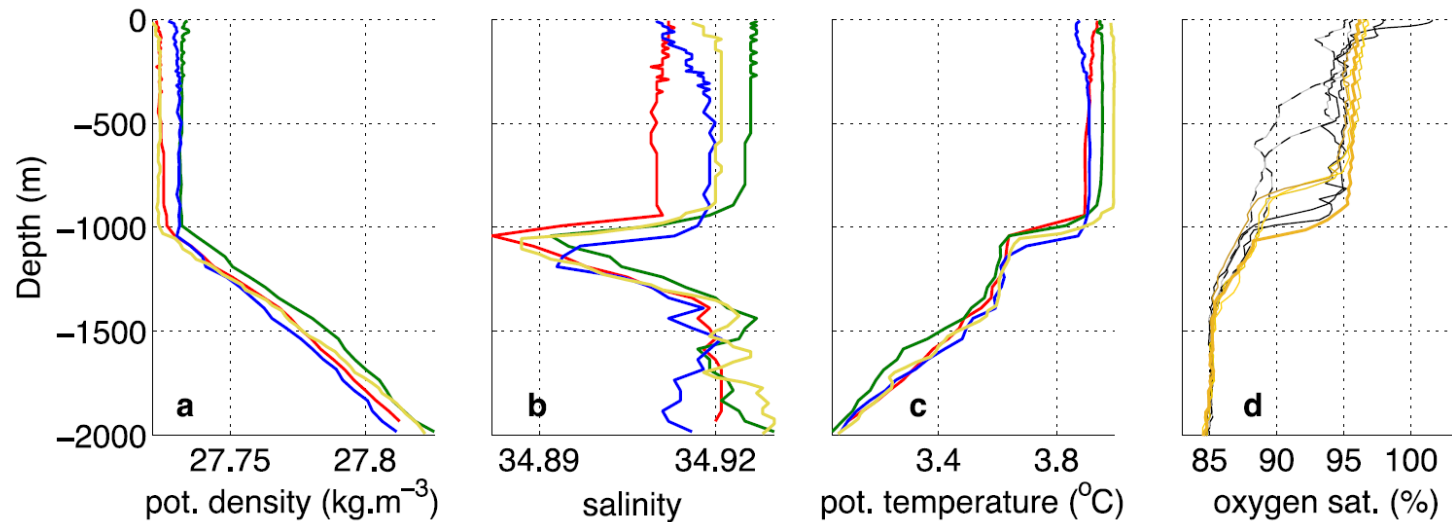


The paradigm of upright deep convection

- Mechanism = gravitational instability
- Return to equilibrium = upward transfer of buoyancy by mixed layer deepening
- Signature = homogeneous hydrological profile + convective plumes

Deep convective profiles in the Irminger Sea (winter 2012, ARGO)

Piron et al 2016

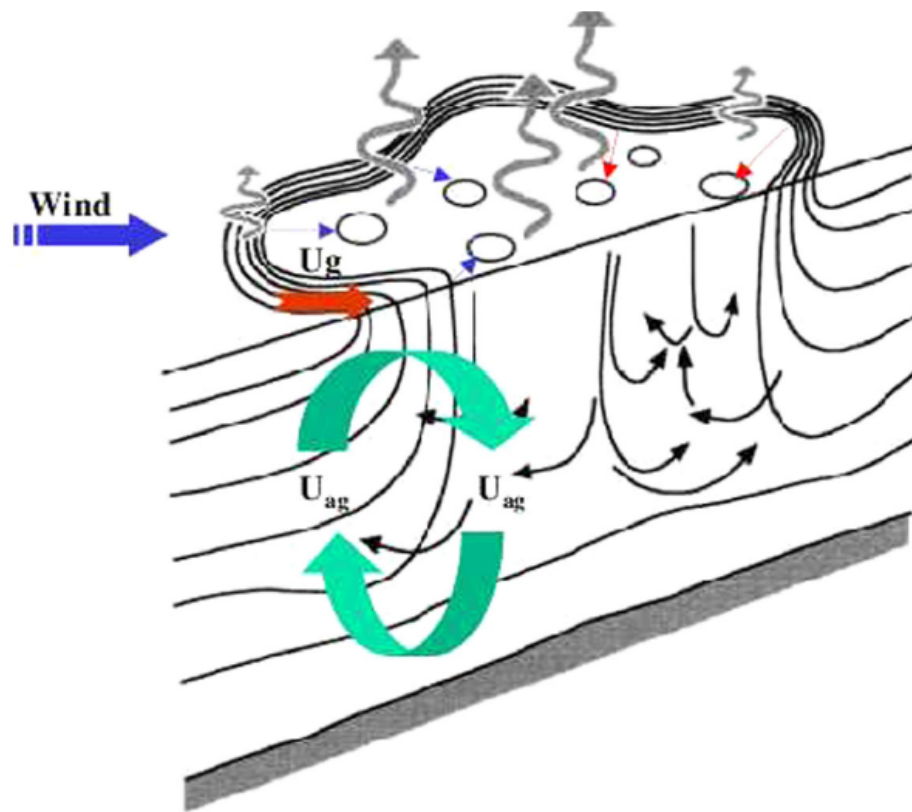


The alternative view of slantwise deep convection

- Mechanism = symmetric instability
- Return to equilibrium = upward transfer of potential vorticity by a slantwise ageostrophic circulation

Scheme of slantwise deep convection

Adapted from Giordani et al 2016



The alternative view of slantwise deep convection

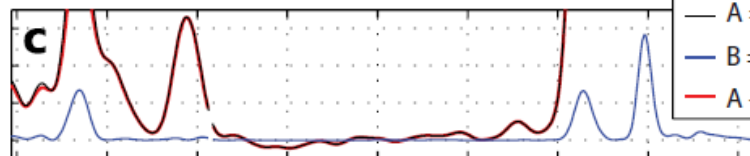
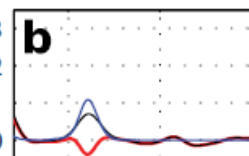
- Mechanism = symmetric instability
- Return to equilibrium = upward transfer of potential vorticity by a slantwise ageostrophic circulation
- Signature = homogeneous water properties along isopycnals + negative horizontal potential vorticity

Slantwise deep convection profiles in the Northwestern Mediterranean Sea (winter 2013, glider)

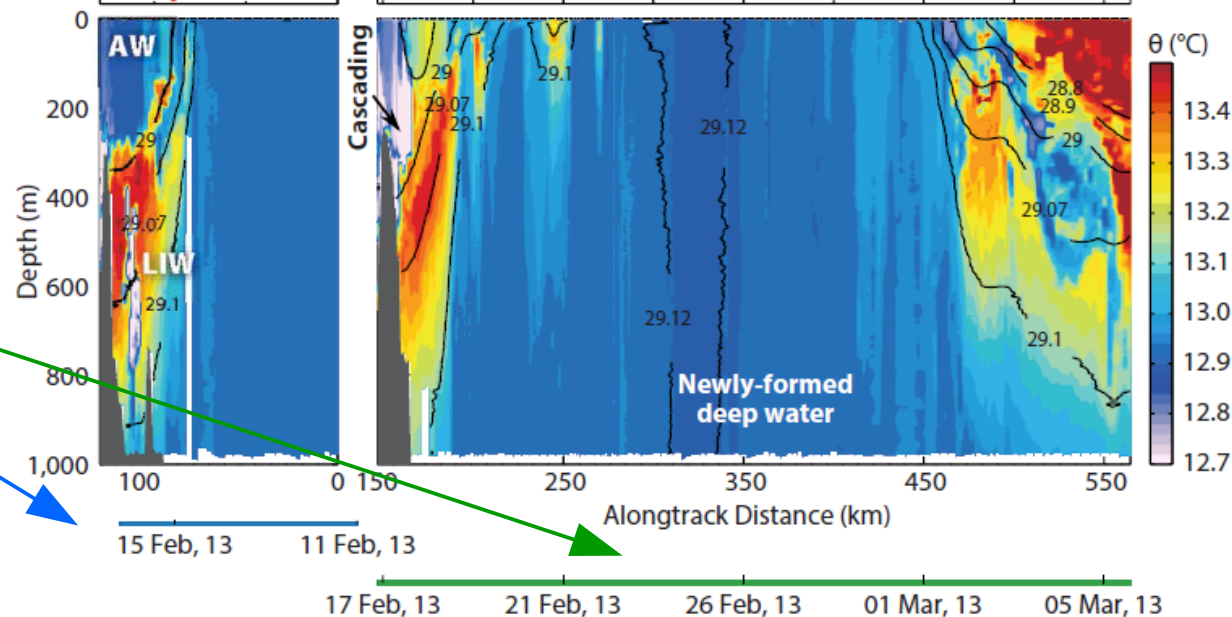
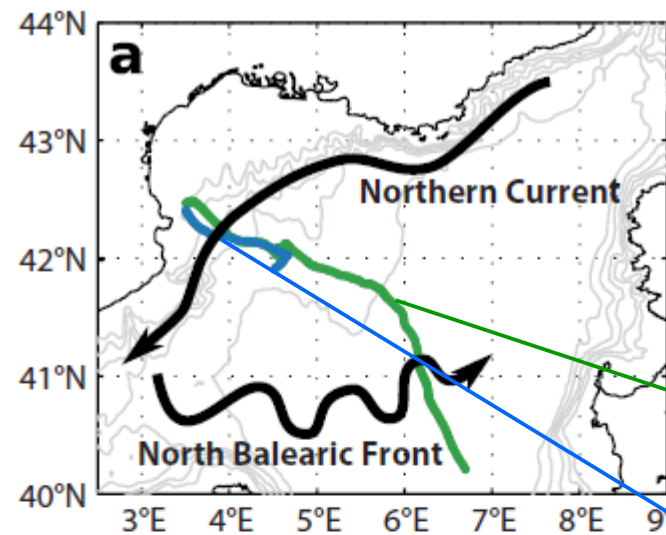
Estournel et al 2016

50-100m geostrophic PV

$\times 10^{-14} (\text{s}^{-4})$



— $A = N^2 f^2$ + vertical
— $B = (db/dx)^2$ - horizontal
— $A - B$ total



15 Feb, 13 11 Feb, 13 17 Feb, 13 21 Feb, 13 26 Feb, 13 01 Mar, 13 05 Mar, 13

Scientific questions

- 1) How do surface forcings of deep convection compare between the Irminger and Mediterranean Seas?
- 2) Do surface forcings favour upright or slantwise deep convection in these basins?

Data

- Daily, 2000-2015
- AVISO (Ssalto/Duacs) gridded SLA, surface \mathbf{u}_g ($1/4^\circ$, Cartesian grid)
- ERA-INTERIM reanalysis (T255 ~ 80km resolution): Fnet, E-P, τ_0 , SLP

Diagnosed surface conditions

- Circulation:

SLA, \mathbf{u}_g

- Surface buoyancy flux:

$$B_\theta = (g \alpha_\theta) / (\rho_0 c_w) F_{net}$$

$$B_s = g \beta_s S (E - P)$$

$$B = B_\theta + B_s$$

- Surface potential vorticity flux:

1) Diabatic:

$$J_z^D = \frac{g(f + \zeta)}{\rho_0 h} \left(\frac{\alpha F_{net}}{C_p} - \beta \rho_0 S (E - P) \right)$$

2) Frictional:

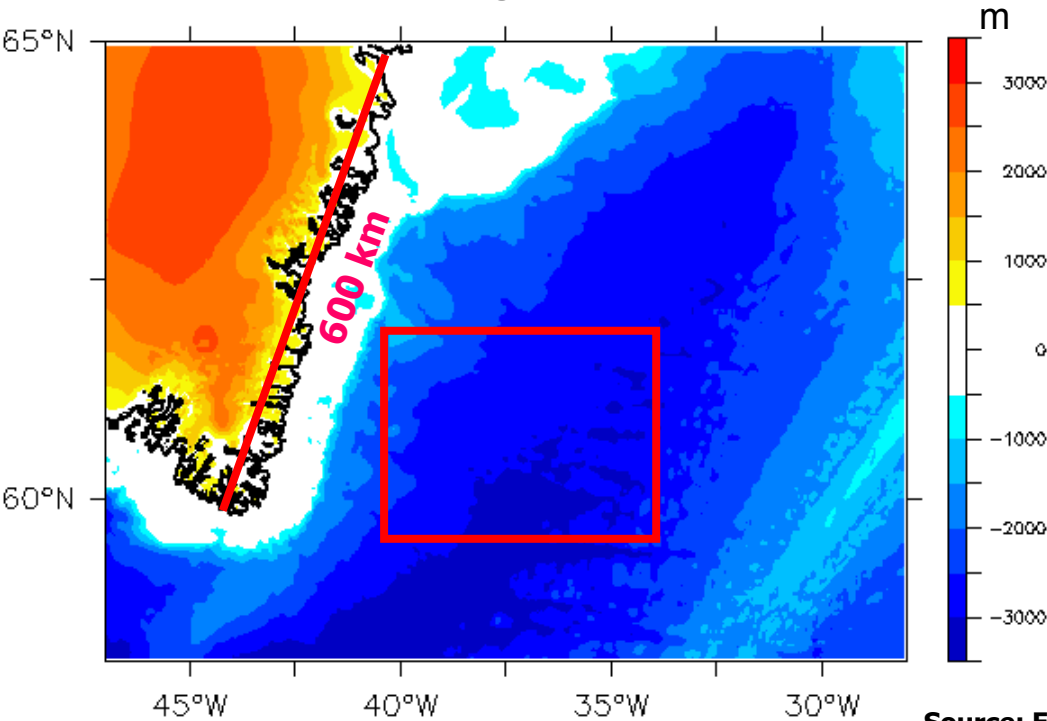
Wind Energy Flux WEF = $\mathbf{u} \cdot \boldsymbol{\tau}_0 / \rho_0$

$$J_z^F = \frac{f}{\rho_0} \frac{\partial \mathbf{U}_g}{\partial z} \cdot \frac{\partial \boldsymbol{\tau}}{\partial z}$$

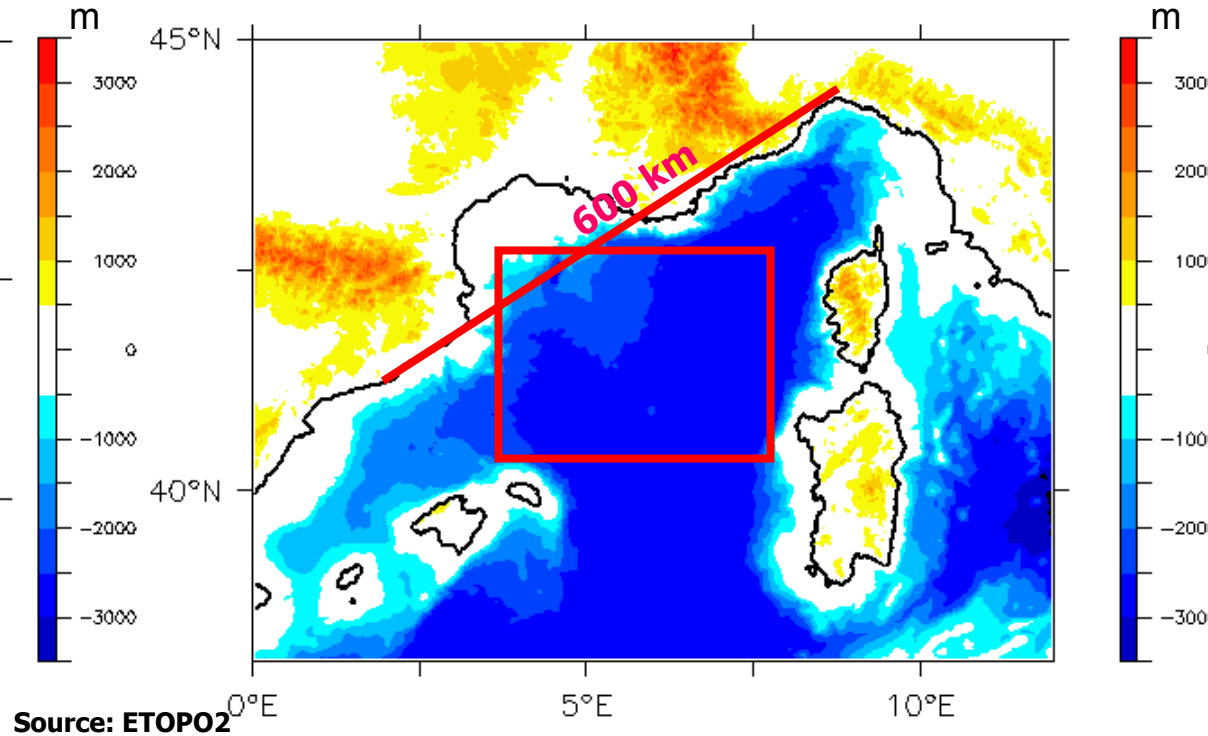
Hypotheses: $(\mathbf{u}, \zeta) \sim (\mathbf{u}, \zeta)_{g+e}$ $h \sim H$ $\frac{\partial \mathbf{U}_g}{\partial z} \sim \frac{\mathbf{U}_g}{H}$ $\frac{\partial \boldsymbol{\tau}}{\partial z} \sim \frac{\boldsymbol{\tau}_0}{h_e}$ (h_e from Cushman-Roisin 1987)

Topography

Irminger Sea



Northwestern Mediterranean Sea

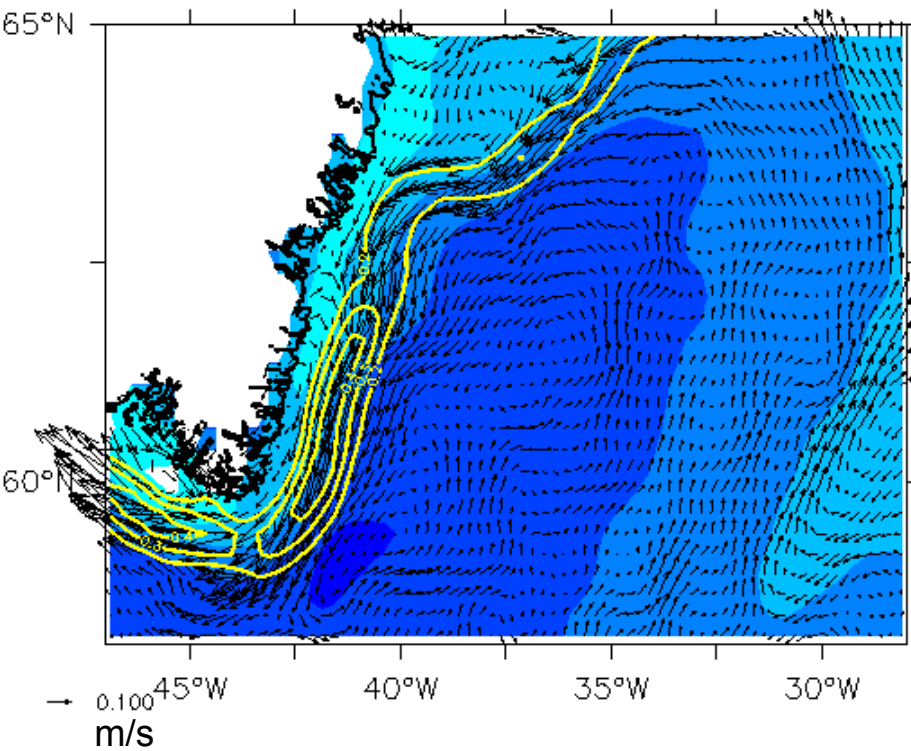


- Similarities: NE-SW basin orientation; partly sloping bathymetry; continental bounding to the NW
- Contrasted continental topography

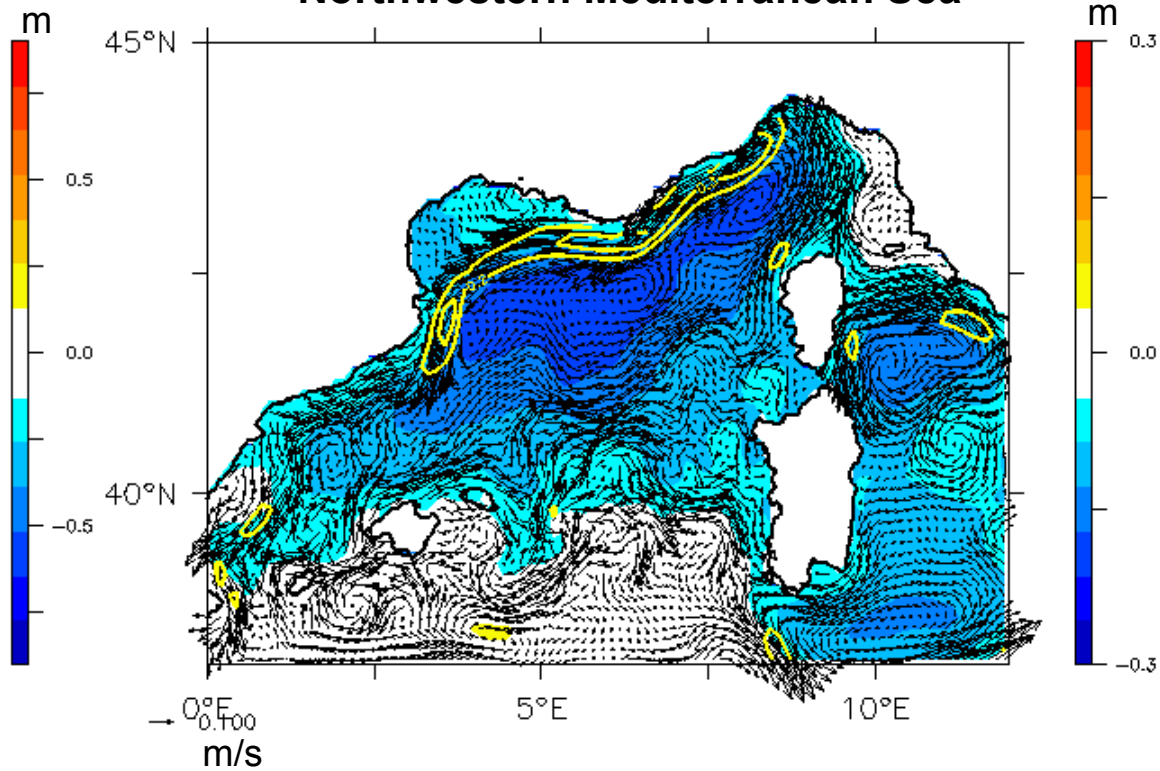
Surface circulation

Winter average SLA (shades) and u_g (arrows and contours)

Irminger Sea



Northwestern Mediterranean Sea

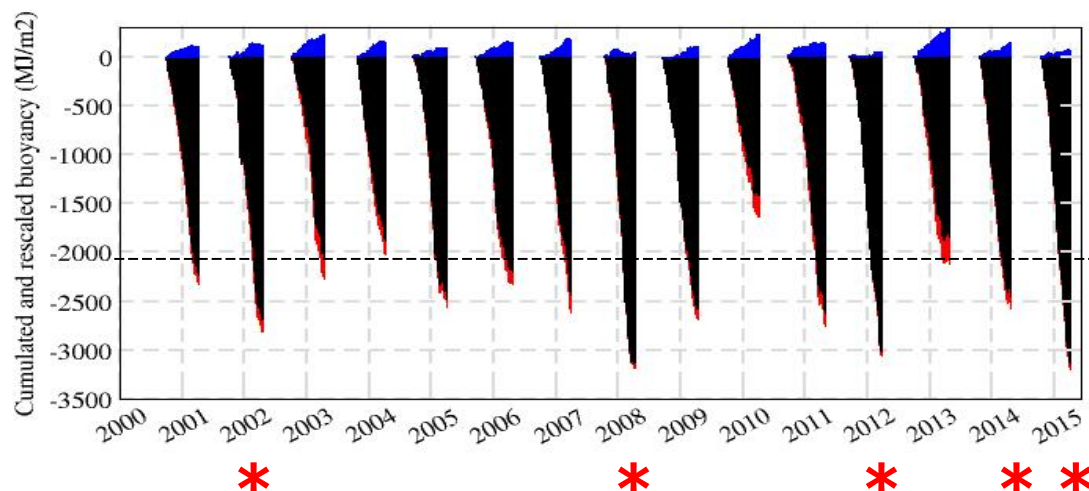


→ Similarities: cyclonic circulation; intense boundary current oriented NE-SW and stabilized by the bathymetry slope

Buoyancy budget

Cumulated winter surface buoyancy budget (rescaled in W/m^2)

Irminger Sea



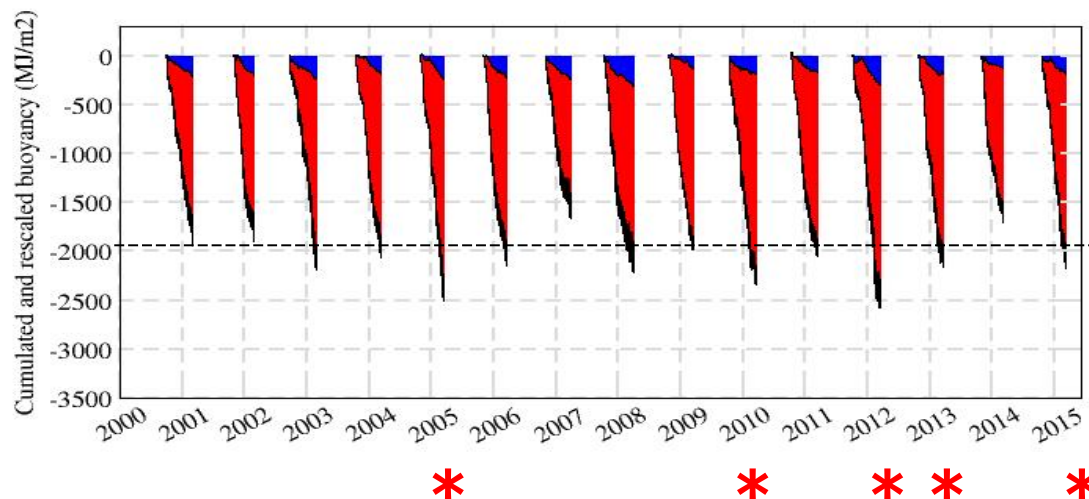
$$B_s = +124 \text{ MJ.m}^{-2}$$

$$B = -2417 (\pm 486) \text{ MJ.m}^{-2}$$

$$B_\theta = -2541 \text{ MJ.m}^{-2}$$

* * * * * Deep convective winters

Northwestern Mediterranean Sea



$$B_s = -208 \text{ MJ.m}^{-2}$$

$$B_\theta = -1896 \text{ MJ.m}^{-2}$$

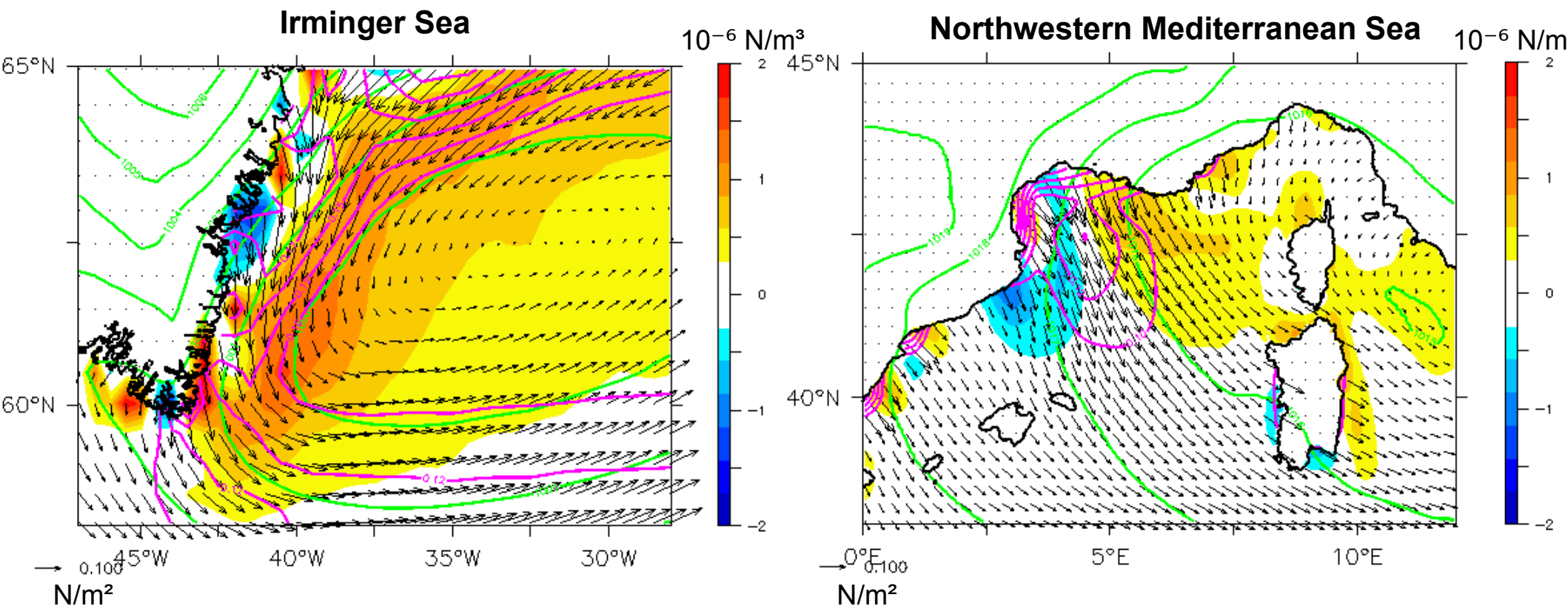
$$B = -2104 (\pm 256) \text{ MJ.m}^{-2}$$

* * * * * Deep convective winters

- Similarities: buoyancy budget dominated by heat loss; deep convection when strong values
- Opposite contribution of the water budget

Wind stress

Winter average wind stress (arrows and magenta contours), wind stress curl (shades) and sea level pressure (green contours)

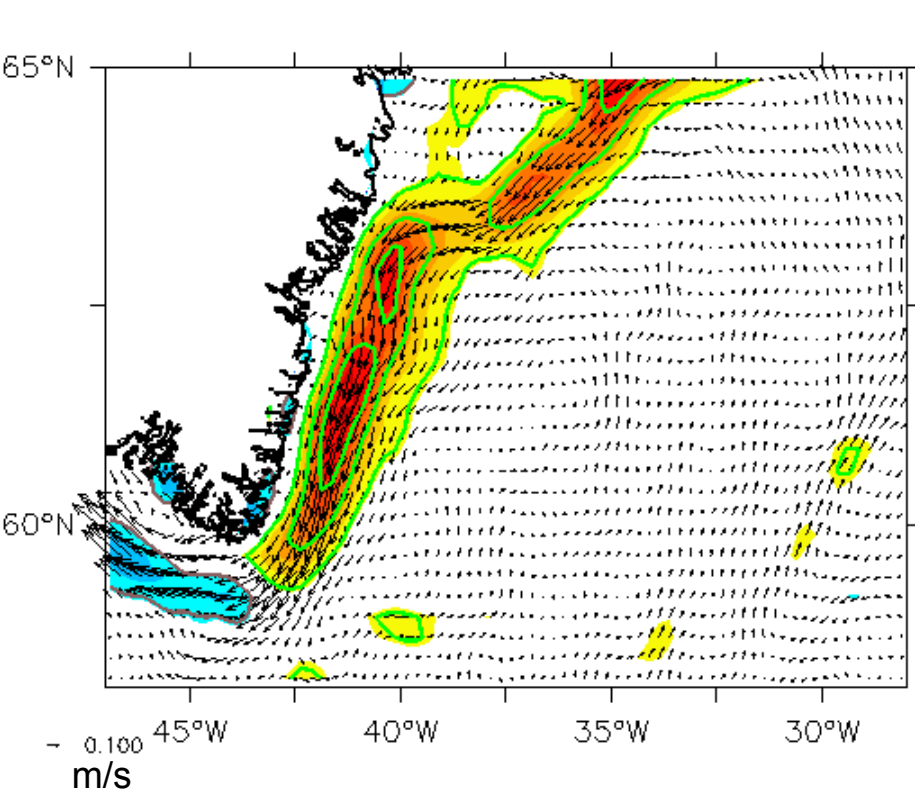


- Similarities: low SLP over sea and high SLP over land
- Very contrasted wind direction: topographic blocking in Irminger Sea and Venturi effect in Northwestern Mediterranean Sea

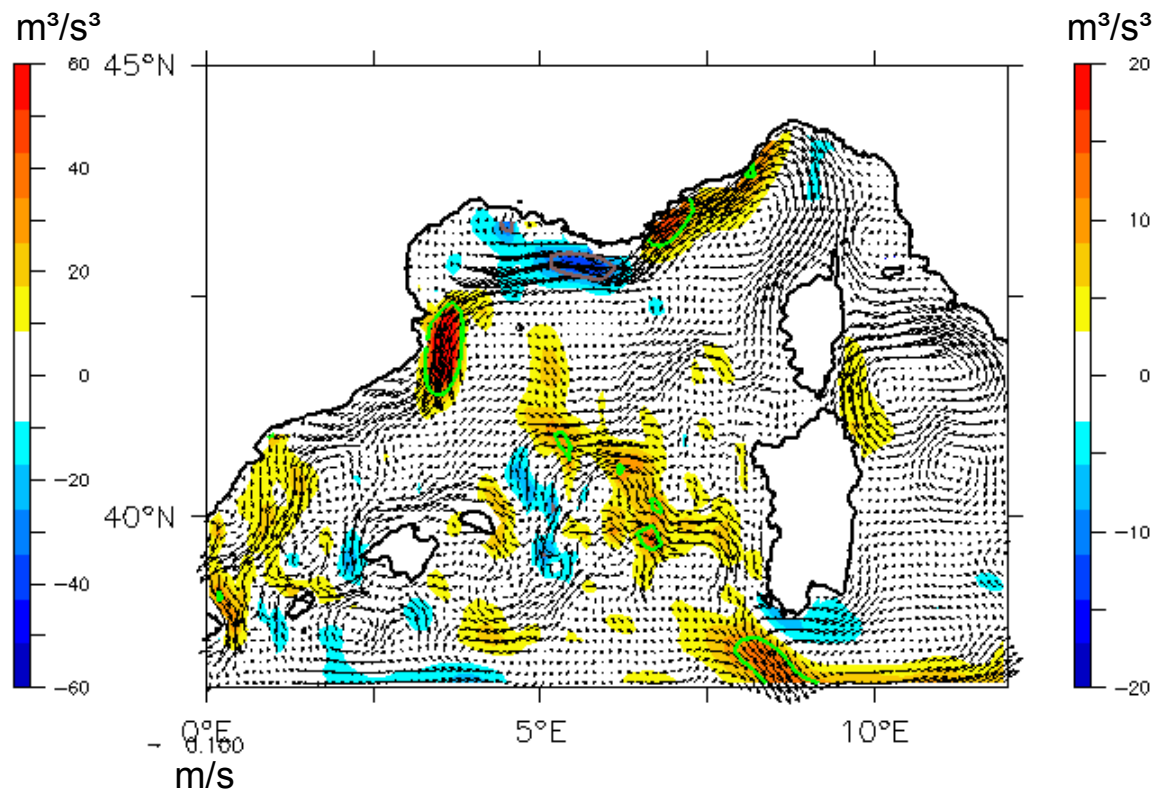
Wind energy flux (WEF)

Winter average WEF (shades), $u_g + u_e$ (arrows) and cosine between current and wind stress (contours)

Irminger Sea



Northwestern Mediterranean Sea

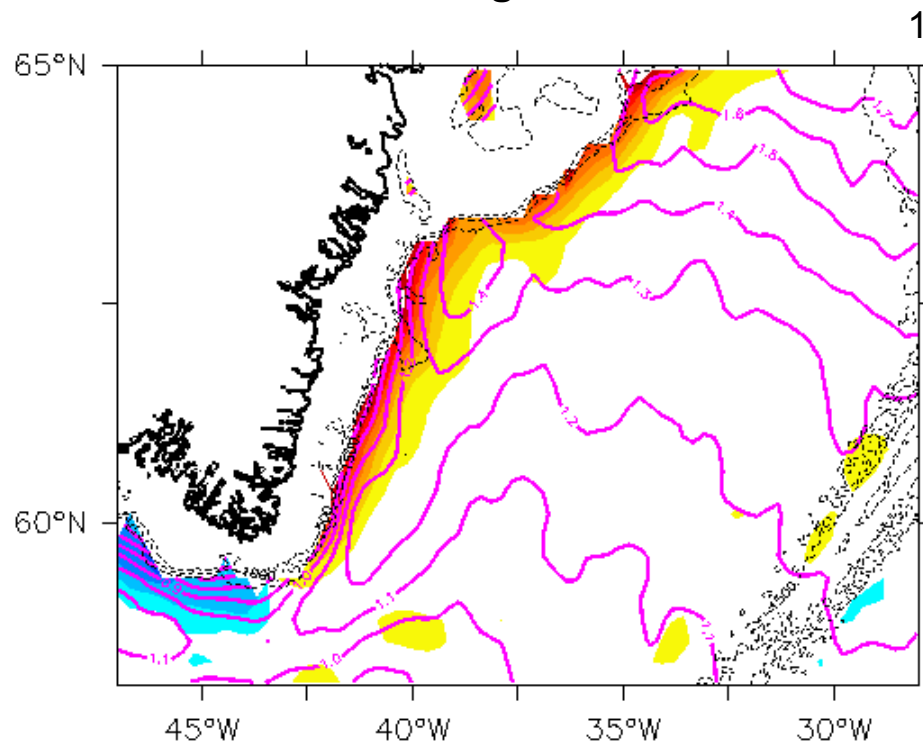


- Similarities: the WEF is highest along boundary currents
- Very contrasted spatial pattern of WEF: positive throughout the East Greenland Current, changing sign along the Northern Current

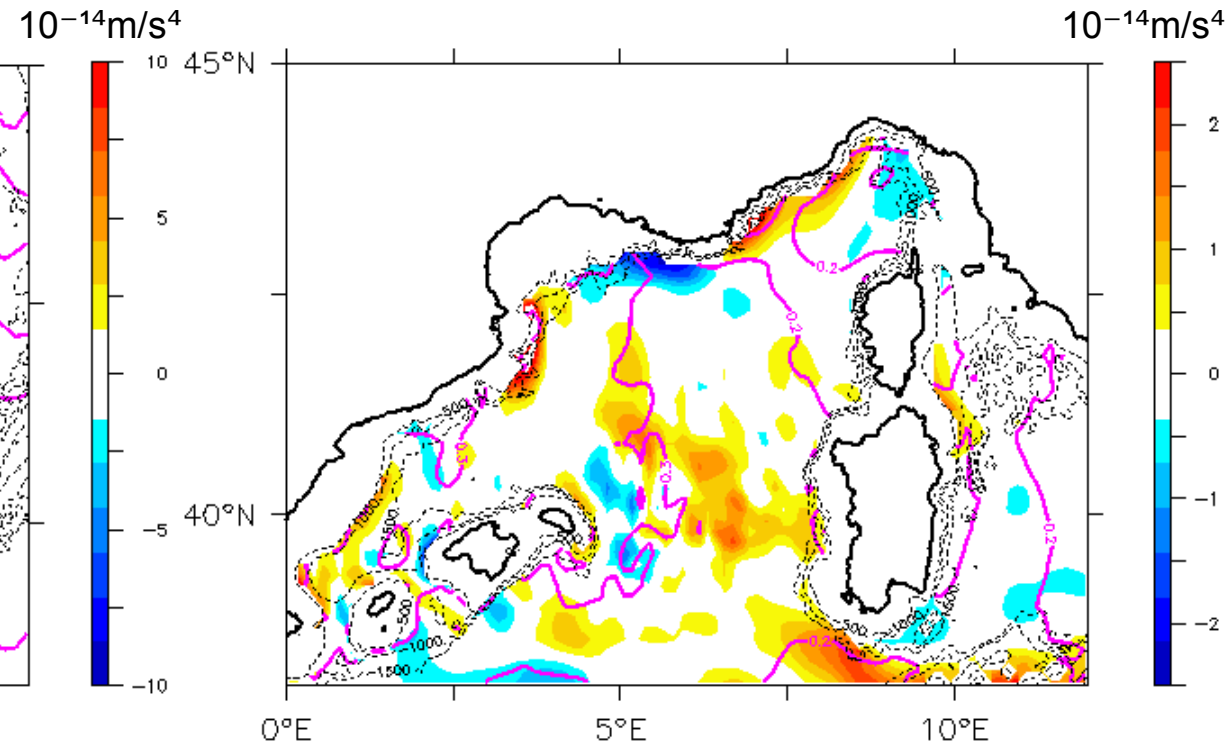
Surface potential vorticity budget

Winter average surface frictional (shades) and diabatic (contours) potential vorticity fluxes

Irminger Sea



Northwestern Mediterranean Sea



- The Northwestern Mediterranean Sea is dominated by the diabatic forcing: mostly upright convection?
- The Irminger Sea undergoes an intense frictional forcing along the East Greenland Current: large contribution of slantwise convection?

Main results

- Both regions display a similar basin-scale circulation: cyclonic gyre and intensified slope boundary current to the NW
- Buoyancy budgets:
 - Are dominated by heat fluxes
 - Explain well the interannual variability of deep convection
 - But opposite contribution of the water budget between basins
- The surface wind is driven by the surrounding continental topography and displays fundamental differences:
 - Colinear (Irminger) vs orthogonal (Mediterranean) to the main boundary current
 - Source of Wind Energy Flux only in the Irminger Sea
 - Potential source of significant slanting deep convection only in the Irminger Sea

Main results

- Both regions display a similar basin-scale circulation: cyclonic gyre and intensified slope boundary current to the NW
- Buoyancy budgets:
 - Are dominated by heat fluxes
 - Explain well the interannual variability of deep convection
 - But opposite contribution of the water budget between basins
- The surface wind is driven by the surrounding continental topography and displays fundamental differences:
 - Colinear (Irminger) vs orthogonal (Mediterranean) to the main boundary current
 - Source of Wind Energy Flux only in the Irminger Sea
 - Potential source of significant slanting deep convection only in the Irminger Sea

Future prospects

- Estimate the surface potential vorticity in order to calculate deep water formation rates in the potential vorticity space (adapting Walin 1977):

$$\tau(q) = \frac{1}{\Delta q \Delta t} \int_t^A \iint_{q-\Delta q/2 < q' < q+\Delta q/2} (J_z^F h_e + J_z^D h) dx dy dt$$

- Characterize from eddy-resolving models the properties of upright vs slantwise convective deep waters
- Link to the AMOC / Mediterranean Thermohaline Circulation (MTHC)?